STUDY OF BIO SORBENTS BY BOTTOM UP APPROACH AND THEIR APPLICATIONS FOR THE TREATMENT OF SIMULATED DYES WASTE WATER

Abstract

Environmental contamination is one of the burning issues of today's world. Pollution not only causes environmental changes but also causes different diseases. Textile effluent is a major contributor of water pollution. Marine lifespan, environment and our ecosystem are affected severely by the disposal of dyes from industries into the receiving water. The objective of this research is adsorption, thermodynamics and kinetic studies of two different organic dyes onto abundantly available inexpensive adsorbents like *Phoenix dactylifera* (date pits), *tea waste biomass* (tea leaves), *Zea covering* (corn husk) and *Prunus persica pits* (peach seeds) for the elimination of acidic (Congo red) and basic (Malachite Green oxalate) dyes from solutions. Selected adsorbents have high surface reactivity and adsorption capability to eliminate malachite green oxalate dye and Congo red dye respectively from simulated waste water system. All natural adsorbents were originate to be reliant on contact time, dye concentration and dose of adsorbent by using spectrophotometric technique before and after dye adsorption. Maximum adsorption of date pits occurred in 20 min with percentage removal of 96.3 %, maximum adsorption of tea leaves ensued in 30 min with 94.23%, extreme adsorption of peach seed powder happened in 40 min with 95.48%, the best adsorption of corn husk arisen in 40 min with 94.40%. The percentage dye removal would decrease with increase in dye concentration, whereas the adsorption capacity of adsorbents will increase with increase in the dye concentration.. The investigational data fitted well to pseudo second order kinetics model and have a Regression coefficient value of 0.999 approximately. Values of percentage removal and K_D for all the adsorbents and dyes systems were also determined at temperatures ranging from 298K to 318K. The adsorption isotherms like Langmuir and Freundlich were employed and the values of respective constants were calculated to estimate the adsorption characteristics. Several thermodynamic parameters like $\Delta G°$, $\Delta H°$ and $\Delta S°$ were also calculated and it was observed that adsorption is spontaneous and endothermic. Pseudo-second order simulations were used to define the dyes adsorption kinetics. The adsorption equilibrium data were fitted well to adsorption isotherm models and proved the pseudo-second order adsorption kinetics. The surface

morphology of adsorbate and adsorbent was resolute by SEM technique of Jeol Japan with model number JSM 6380A. The liquid phase is then analysed for the equilibrium concentration Ce of the chemical in aqueous solution. **K_D (the adsorption–desorption coefficient)** values are determined over a range of concentrations at a constant temperature. The resultant plot is termed an **adsorption** "isotherm", which can take a number of shapes as illustrated below from figure 1 to 8.

INTRODUCTION

Chemicals are the outline of contamination into the natural environment which is the reasoning of adverse variation. It may yield the usage of chemical substances or energy, such as heat, noise and light. Contaminants are the constituents of environmental pollution [1]. Effluence is categorized as point source or nonpoint source pollution. Environmental detoxification has been progressed and it is a basic focus of apprehension for all the humans globally [2]. There are many forms of pollution, the air we use for the breathing, drinking water, the land where we grow our crops and even the noise of vehicles we hear every day, all these subsidize to human health glitches [3]. Water pollution is one of the biggest apprehension among all the environmental contaminations. Waste water treatment technologies are not present in poor and developing countries therefore they are at the high risk [4]. Domestic activities, modern agricultural practices, mining activities, municipal wastes, marine dumping, radioactive wastes, oil spillage, underground storage leakages and industries are polluting the aquatic system. Different industrial units are the major culprits causing the pollution of water resources. Wide range of industries discharges the toxic chemicals through effluents (i.e. tanneries industries, industry of canneries, refining industries, mines, fertilizers production entities, textile, steel, oil, detergent production units, electroplating units and sugar refines) into water bodies contaminates these possessions and causes hazardous effects on marine life. Organic toxic waste initiates from industrialized effluents, management plants like food processing, pulp and paper making, aquaculture, home sewage and agriculture contaminated water. Countless rate of liquefied oxygen in the receiving water is consumed during the disintegration procedure of pollutants [5]. Large quantities of suspended solids are present with organic pollutants, decrease the light feasibility to photosynthetic creatures and rendering it an inappropriate habitat for numerous

invertebrates [6]. Examples of Organic pollutants are fertilizers, hydrocarbons, phenols, plasticizers, biphenyls, detergents, oils, pharmaceuticals, proteins, greases and carbohydrates [7-9].

EXPERIMENTAL SECTION

Preparation of Malachite green oxalate and Congo red dye Solutions

Dye solution of congo red was prepared by using double distilled water. The absorbance of respective concentrations of dye was measured by UV-Visible spectrophotometer of Jeol Japan with model number EX-54175JMU displays a penetrating peak in diluted concentration of dye around 498 nm in aqueous solution. Molar extinction coefficient of congo red is approximately 45000 l/mol.cm. Similarly Malachite green oxalate dye displays a penetrating peak in diluted concentration of dye around at wavelength 621 nm and its molar extension coefficient is $1*10^5\ M^{-1}cm^{-1}$ [10].

Preparation of natural adsorbents

Peach seed of 100 nm in size were collected, washed by deionized water and dried at ambient conditions. The mixture of dried peach seed covers were grounded separately by house mill to prepare powders with different particle sizes by using a standard sieves set and used for the removal of malachite green oxalate dye.

We took corn husk from the tree of north nazimabad, Karachi, Pakistan and it washed many times from double distilled water to remove impurities and dust from it. The washed husk, 100 nm in size was dried in an oven at 390 K for 2 days, after complete drying it was grounded about 100 to get a minimum size.

We obtained the tea leaves 100 nm in size from the northern area of Karachi, Pakistan. Used tea leaves were washed numerous times by double distilled water till they become clear and completely colorless and then they dried in an oven dried for 3 days at 80 °C. The dried leaves were grounded to get a particle size of 120-260 mm and the sieved leaves were stored in a sealed bottle for experimentation.

The date pits, 100 nm in size were obtained from dates. As sample contained variable amount of date pits waste material and it dissolve in deionized water and then dry in air.

Optimization of Adsorbent Dosage

For the analysis of maximum adsorption, which occurs at the ideal amount 100nm size of peach seeds, experimentation was accomplished. For this tenacity, 30.0 ml of MGO dye with concentration 3×10^{-5} mol.dm^{-3} was taken, different amount was taken from 0.1g -1.2g. All the flasks were placed on shaking in a thermostat shaker for 30 min. After the shaking all the flask were filtrated out by Wattman filter paper and first 10 ml of filtrate was thrown away. Filtrate of each flak examined by UV visible spectrophotometer for detecting absorbance after adsorption process of each solution.

Dissimilar amount of corn husk from 0.1g-1.2g were measured and put into the conical flask having 30ml of $5x10^{-5}$M solution of MGO dye and placed at the hot plate for 30 minutes. After 30minutes final absorbance was examined by UV-visible spectrophotometer for measuring the absorbance of solution at 617 nm. In this way the value of finest amount was determined at which extreme adsorption occurred.

1×10^{-5} M solution was prepared. Different amount of tea leaves waste 0.1g to 0.8g was measured and placed in respective conical flasks. 25ml of $1x10^{-5}$M solution was drawn in the flask. After 30min final absorbance was analyzed by UV visible spectrophotometer at 496nm. In this way ideal amount was determined at which extreme adsorption occurred.

Determination of Stay Time

For analyzing the optimum trembling time, taken 50.0ml of dye solution in shaking flask and the augmented quantity of MgO nanoparticles were added in each flask. The shaking time was varied from 10 to 120 min for MGO and 15 to 240 min for CR. After specific interval of time content of each flask was strained, the absorbance of the filtrate was noted down using ultraviolet visible Spectrophotometer. Optimum shaking time of adsorbent was determined by finding K_D and percentage removal values [11].

For determining the maximum time of adsorption for each natural adsorbent, 30ml with 3×10^{-5} mol.dm^{-3} for the powder of peach seeds cover and dye solutions were taken out in reagent bottles. Best amount of adsorbent was taken which was determined in preceding experiment in

every flask. These flasks were placed in a shaking incubator and after every 5 minutes one bottle was removed from the incubator. Solution was filtered and examined with UV visible spectrophotometer in order to recognize absorbance of solution after dissimilar shaking time intermissions. Optimal shaking time for the adsorption was 30 minutes for all bottles.
Optimized amount of corn husk 0.5g was measured and put into the conical flask with 30ml of $5x10^{-5}$ M solution concentration of malachite green for different time interval after respective particular time, final absorbance was measured at 617 nm. The time where maximum adsorption occurred was taken as optimum time for adsorption.

Optimum amount of tea leaves waste 0.5 g was measured and placed in column with 30ml of $1x10^{-5}$M concentration solution of congo red for different time of interval after respective particular time. Final absorbance was measured at 496nm. The time where maximum adsorption occurred was taken as optimum time for adsorption.

Optimum amount of date pits waste 0.6 gm was measured and placed in column with 30ml of $1x10^{-5}$M concentration solution of Congo red for different time of interval after respective particular time. Final absorbance was measured at 496nm. The time where maximum adsorption occurred was taken as optimum time for adsorption.

Optimization of Concentration of Adsorbate

Working standard of dye solutions were prepared by varying the concentrations of 50ml of each nano particle solution and 30ml of each of natural adsorbents were taken in separate flask and optimized amount of adsorbent was added in respective flask and kept them in shaking incubator by keeping optimized time at 303K temperature. After optimized time the contents were filtered out and absorbance of each the content was measured at their respective λ_{max}. The optimum range of concentration of MGO and CR dyes were selected for further studies [12].

TABLE 1: ANALYSIS OF AMOUNT

Optimization of Amount for the Elimination of Congo Red Dye by Using Tea leaves powder			
Amount(g)	Equilibrium Conc.x10^6	% Removal	K_D
0.1	2.933	93.139	1.761
0.2	1.842	77.452	1.751
0.3	9.111	78.690	1.822
0.4	4.066	90.488	0.612
0.5	7.601	82.224	0.912
0.6	9.602	77.546	0.961
0.7	2.977	93.035	0.255
0.8	2.466	94.230	0.185
Optimization of Amount for the Elimination of Congo Red Dye by Using Date pits powder			
Amount(g)	Equilibrium Conc.x10^7	% Removal	K_D
0.1	0.213	67.123	128
0.2	6.888	89.383	20.666
0.3	0.153	76.369	30.666
0.4	0.106	83.561	16
0.5	3.333	94.863	4
0.6	2.444	96.232	2.444
0.7	6.444	90.068	5.523
0.8	7.555	88.356	5.666
0.9	4.222	93.493	2.814
Optimization of Amount for the Removal of MGO Dye by using Corn Husk powder			
Amount(g)	Equilibrium Conc.x10^6	% Removal	K_D
0.1	1.712	89.579	10.275
0.3	1.141	93.052	2.283
0.5	9.200	94.401	1.104
0.7	1.423	91.336	1.220
0.9	1.920	88.312	1.280
1.2	1.631	90.069	0.815
Optimization of Amount for the Removal of MGO Dye by Using Peach seeds shell powder			
Amount(g)	Equilibrium Conc.x10^6	% Removal	K_D
0.1	0.210	89.605	4.905
0.3	0.152	90.134	5.081
0.5	8.193	94.697	1.638
0.7	7.051	95.436	1.007
0.9	8.193	94.697	0.910
1.2	6.984	95.480	0.582

TABLE 2: ANALYSIS OF TIME

Optimization of time for the Elimination of CR Dye by Using Tea leaves powder				
Amount(g)	Time (min)	Equilibrium Concentration(Ce)x10^6	% Removal	K_D
0.5	10	1.991	53.430	2.389
0.5	15	4.933	88.461	0.592
0.5	20	1.468	65.644	1.762
0.5	25	4.888	88.565	0.586
0.5	30	2.466	94.230	0.296
0.5	35	2.133	95.010	0.256
0.5	40	2.111	95.062	0.253
0.5	45	2.133	95.010	0.256
Optimization of time for the Removal of CR Dye by Using Date pits powder				
Amount(g)	Time (min)	Equilibrium Concentration(Ce)x10^7	% Removal	K_D
0.6	10	6.889	89.383	6.888
0.6	15	5.333	91.780	5.333
0.6	20	1.776	97.260	1.777
0.6	25	2.221	96.575	2.222
0.6	30	2.454	96.232	2.444
0.6	35	1.911	70.547	19.111
0.6	40	1.012	81.506	12.000
0.6	45	9.551	85.273	9.555
0.6	50	4.667	92.808	4.666
Optimization of time for the Removal of MGO Dye by Using Corn husk powder				
Amount(g)	Time (min)	Equilibrium Concentration(Ce)x10^6	% Removal	K_D
0.5	10	1.296	92.112	1.555
0.5	15	1.182	92.807	1.418
0.5	20	1.081	93.420	1.297
0.5	25	1.141	93.052	1.370
0.5	30	9.402	94.278	1.128
0.5	35	1.141	93.052	1.370
0.5	40	8.596	94.769	1.031
0.5	45	8.730	94.687	1.047
0.5	50	1.148	93.011	1.378

Optimization of time for the Removal of MGO Dye by Using peach seeds powder					
S. No.	Amount Of Adsorbent (g)	Time (min)	Equilibrium Concentration Ce (M)x10^7	% Removal	K_D (M)
01	0.7	10	5.104	96.697	0.729
02	0.7	15	4.499	97.088	0.642
03	0.7	20	8.260	94.654	1.1801
04	0.7	25	7.051	95.436	1.007
05	0.7	30	7.051	95.436	1.009
06	0.7	35	5.036	96.740	0.719
07	0.7	40	3.492	97.740	0.498
08	0.7	45	5.439	96.479	0.777

TABLE 3: ANALYSIS OF TEMPERATURE

% Removal of CR dye by Using Tea Leaves at Different Temperatures

Dye	Ci (M) (10^5)	% REMOVAL			
		303K	308K	313K	318K
CR dye	0.1	79.96071	90.56	84.67	79.96
	0.3	88.14383	95.9	98.54	90.53
	0.5	99.45455	93.8	82	65.45
	0.7	71.20448	44.14	96.5	97.47
	0.01	77.37643	81.36	83.4	87.45
	0.003	93.83562	80.46	93.49	72.26

% Removal of CR by Using Date Pits Powder at Different Temperatures

Dye	Ci (M) (10^5)	% REMOVAL			
		303K	308K	313K	318K
CR dye	0.1	93.90	85.46	96.86	97.24
	0.3	70.74	98.2	99.22	96.89
	0.5	92.181	74.18	96.545	96.72
	0.7	91.372	98.03	98.823	99.66
	0.01	85.741	96.38	92.96	96.95
	0.003	94.863	95.27	93.15	91.78

% Removal of MGO dye by Using Corn Husk Powder at Different Temperatures

Dye	Ci (M) (10^5)	% REMOVAL			
		303K	308K	313K	318K
MGO dye	0.1	88.6	91.40	87.94	88.18
	3	92	94.10	93.11	95.45
	5	95	95.30	91.58	89.61
	7	91	91.44	91	90.43
	8	94	95.95	93	93.69
	9	90	90	92.07	99.25

% Removal of MGO dye by Using Peach Seed Powder at Different Temperatures

Dye	Ci (M) (10^5)	% REMOVAL			
		303K	308K	313K	318K
MGO Dye	0.1	95.836	95.970	95.903	96.642
	3	98.522	92.366	98.365	93.082
	5	89.939	98.616	98.186	98.871
	7	95.074	91.269	90.597	91.045
	8	94.224	88.314	94.358	90.463
	9	95.202	91.844	96.450	94.531

TABLE: 4 LANGMUIR ISOTHERMS

Langmuir parameters for used tea leaves powder						
S. No.	Temperature	Intercept	Slope	Constant	Constant	R^2
	K	1/K Vm	1/Vm	K_L	Vm x10^5	
01	303	2.2228	94396	42467.158	1.059	0.005
02	308	1.6251	11680	7187.250	8.516	0.344
03	313	-0.5367	12888	24013.415	7.759	0.738
04	318	0.9372	75764	80840.802	1.319	0.212
Langmuir parameters for date pits powder						
S. No.	Temperature	Intercept	Slope	Constant	Constant	R^2
	K	1/K Vm	1/Vm	K_L	Vm x10^5	
01	303	0.586	21313	36351.697	4.691	0.604
02	308	2.697	46629	17286.005	2.144	0.744
03	313	2.818	13955	4950.512	8.425	0.188
04	318	0.556	9277.2	16682.611	1.077	0.471
Langmuir parameters for prunus persica seeds shell powder						
S. No.	Temperature	Intercept	Slope	Constant	Constant	R^2
	K	1/K Vm	1/Vm	K_L	Vm	
01	303	0.483	0.006	0.01240	166.66	0.0466
02	308	0.151	0.0254	0.1674	39.370	0.7065
03	313	0.331	0.0234	0.070652	42.7350	0.7999
04	318	0.252	0.0294	0.11638	34.0136	0.5833
Langmuir parameters for corn husk powder						
S. No.	Temperature	Intercept	Slope	Constant	Constant	R^2
	K	1/K Vm	1/Vm	K_L	Vm	
01	303	0.238	4792	20100.677	2.086	0.004
02	308	0.168	0.0555	0.330	18.018	0.003
03	313	0.013	0.0012	0.092	8333.330	0.028
04	318	0.127	0.0626	0.497	15.974	0.007

TABLE: 5 FREUNLICH ISOTHERMS

Freundlich parameters for tea leaves powder						
S. No.	Temperature	Intercept	Slope	Constant	Constant	R^2
	K	log k	1/n	K_F x10^4	n	
01	303	-3.212	0.188	6.136	5.302	0.181
02	308	-3.143	0.291	7.189	3.427	0.236
03	313	-3.221	0.194	6.010	5.154	0.289
04	318	-3.687	0.107	2.055	9.302	0.025
Freundlich parameters for date pits powder						
S. No.	Temperature	Intercept	Slope	Constant	Constant	R^2
	K	log k	1/n	K_F x10^4	n	
01	303	-3.2842	0.2823	5.197	3.542	0.445
02	308	-4.7056	0.0155	0.198	64.516	0.003
03	313	-4.4907	0.0836	0.323	11.961	0.055
04	318	-2.9024	0.3074	1.251	3.253	0.443
Freundlich parameters for prunus persica seeds shell powder						
S. No.	Temperature	Intercept	Slope	Constant	Constant	R^2
	K	log k	1/n	K_F x10^3	n	
01	303	0.049	0.9475\	1.121	1.055	0.707
02	308	-2.315	0.460	4.835	2.172	0.436
03	313	-2.814	0.391	1.533	2.556	0.805
04	318	-2.385	0.466	4.114	2.141	0.359
Freundlich parameters for corn husk powder						
S. No.	Temperature	Intercept	Slope	Constant	Constant	R^2
	K	log k	1/n	K_F	n	
01	303	4.652	1.835	44946.926	0.544	0.889
02	308	2.604	1.415	401.883	0.706	0.799
03	313	3.411	1.570	2581.071	0.032	0.895
04	318	-0.409	0.773	2.565	1.292	0.894

TABLE: 6 ADSORPTION KINETICS

Pseudo second order kinetics			
Adsorbents	Intercept	Slope	R^2
Date pits powder	1E+06	2026.3	0.006
Peach seeds powder	-87390	46005	0.712
Grounded Tea leaves	-102615	9140.5	0.887
Grounded Corn Husk	17524	-26456	0.904

TABLE: 7 THERMODYNAMIC PARAMETERS

Samples	T (K)	ΔG° ($KJmol^{-1}$)	ΔH° ($KJmol^{-1}$)	ΔS° ($KJmol^{-1}$)	Ln k	1/T
Tea Leaves	303	-26845.520	-1816.9	16.181	10.656	$3.30x10^{-3}$
	308	-22739.286			8.880	$3.246\ x10^{-3}$
	313	-26247.573			10.086	$3.194\ x10^{-3}$
	318	-29876.154			11.300	$3.144\ x10^{-3}$
Date Pits	303	-26453.500	3318.4	-0.9188	10.502	$3.30x10^{-3}$
	308	-24986.537			9.757	$3.246\ x10^{-3}$
	313	-25542.153			9.815	$3.194\ x10^{-3}$
	318	-25703.852			9.722	$3.144\ x10^{-3}$
Corn Husk	303	-24960.939	52465	-170.4	9.908	$3.30x10^{-3}$
	308	2838.9656			-1.108	$3.246\ x10^{-3}$
	313	6186.4274			-2.382	$3.194\ x10^{-3}$
	318	1876.566			-0.709	$3.144\ x10^{-3}$
Peach Seeds	303	1204.465	-8486.3	25.048	-4.390	$3.30x10^{-3}$
	308	4576.937			-1.787	$3.246\ x10^{-3}$
	313	6896.0183			-2.649	$3.194\ x10^{-3}$
	318	5686.646			-2.150	$3.144\ x10^{-3}$

FIGURES

OPTIMIZATION OF AMOUNT

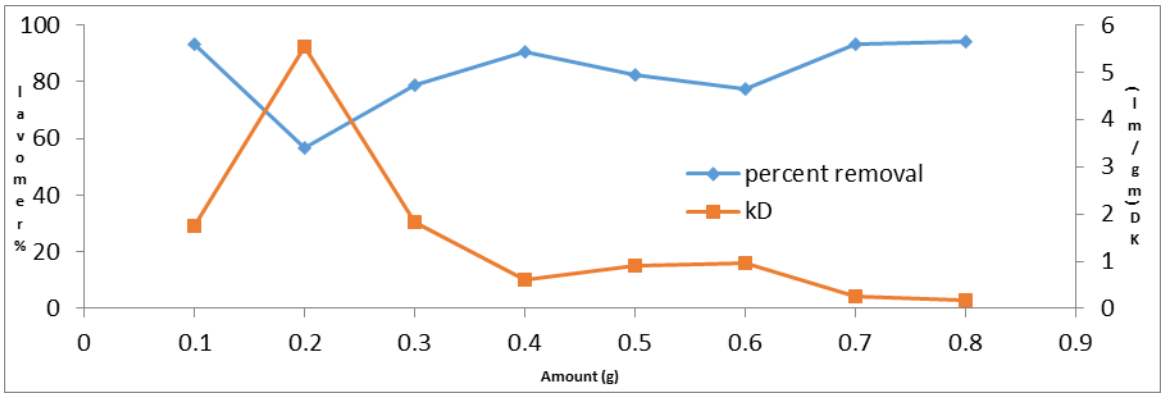

Figure 1: Optimization of amount for elimination of Congo red dye by using used tea leaves powder

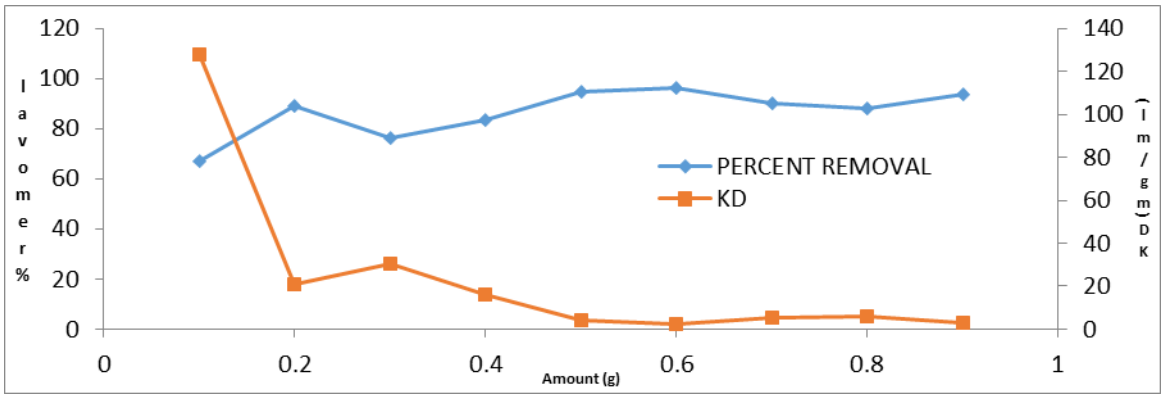

Figure 2: Optimization of amount for elimination of Congo red dye by using date pits powder

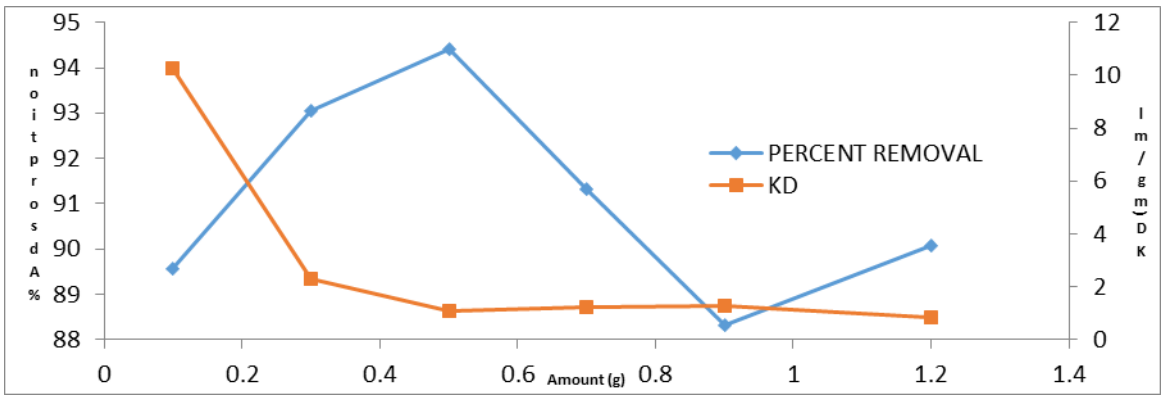

Figure 3: Optimization of amount for elimination of Malachite green oxalate dye by using Corn Husk powder

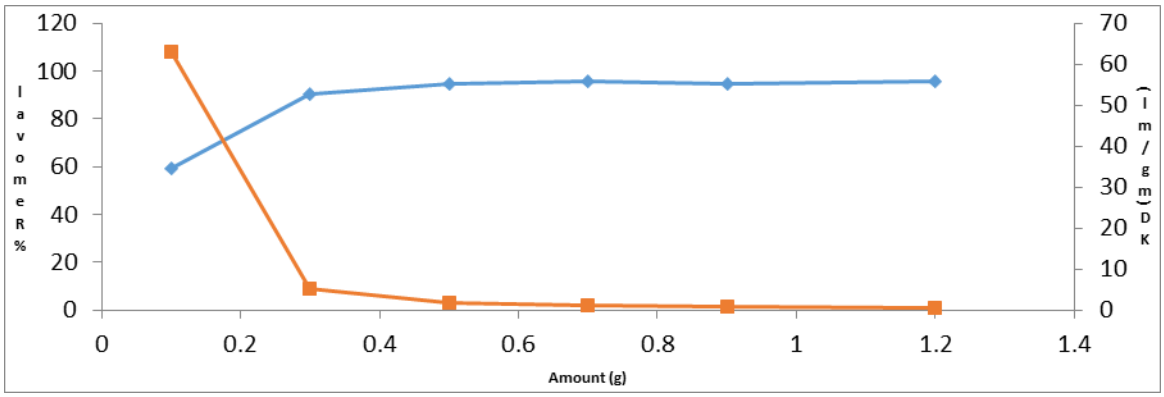

Figure 4: Optimization of amount for elimination of MGO dye by using Peach Seed powder

OPTIMIZATION OF TIME

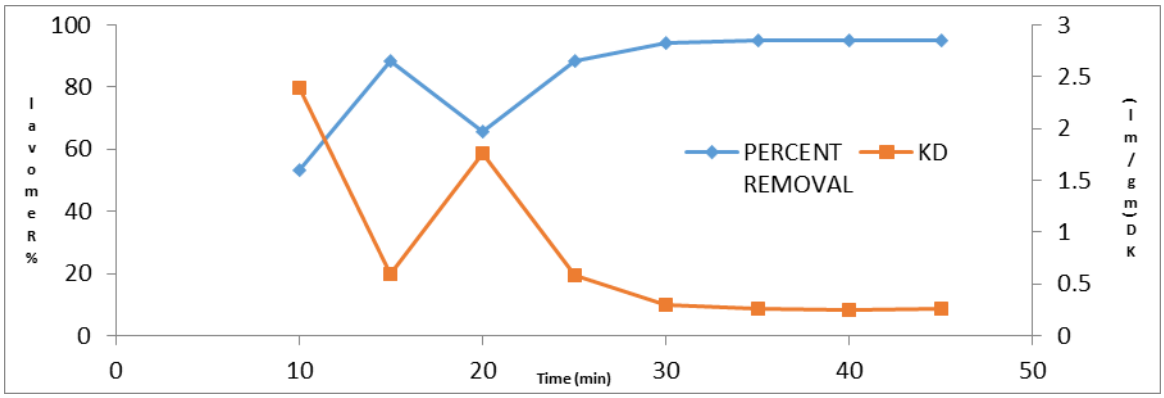

Figure 5: Optimization of time for removal of Congo red dye by using Tea leaves powder

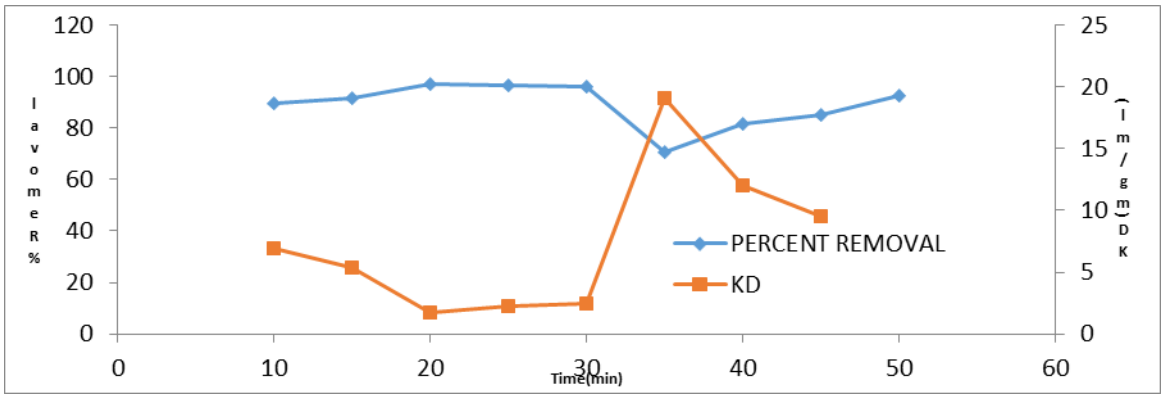

Figure 6: Optimization of time for elimination of Congo red dye by using Date pits powder

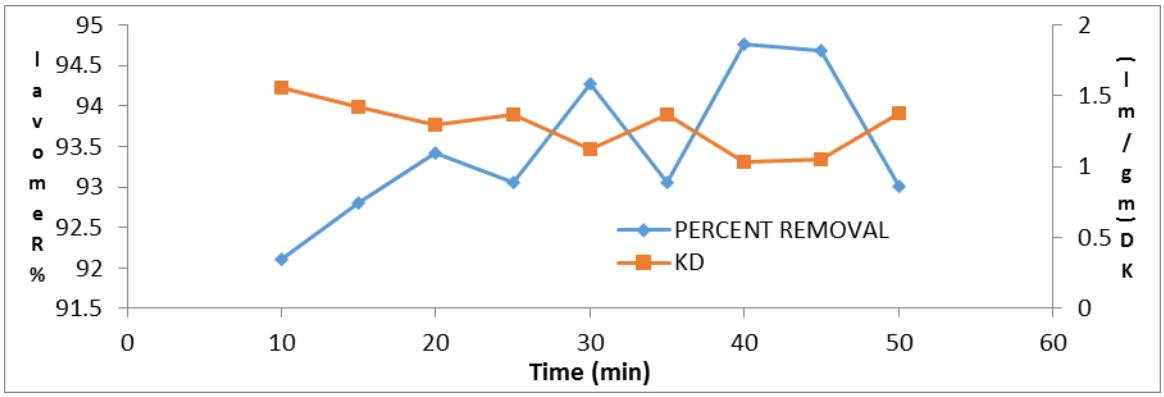

Figure 7: Optimization of time for elimination of Malachite green oxalate dye by using Corn husk powder

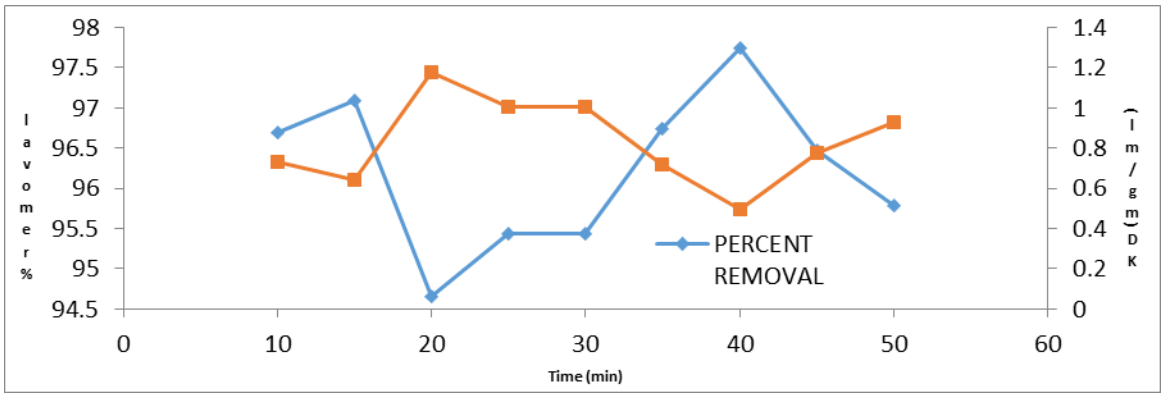

Figure 8: Optimization of time for elimination of Malachite green oxalate dye by using Peach seed powder

LANGMUIR PARAMETERS OF TEA LEAVES

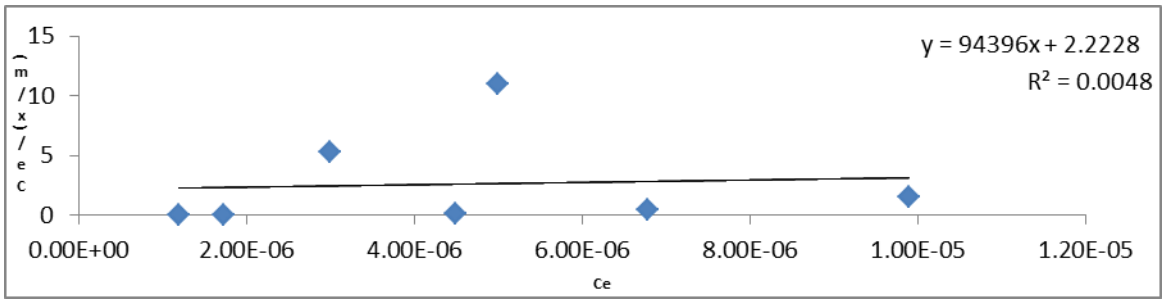

Figure 9: Optimization of Langmuir parameters at temperature 303K of Tea leaves powder

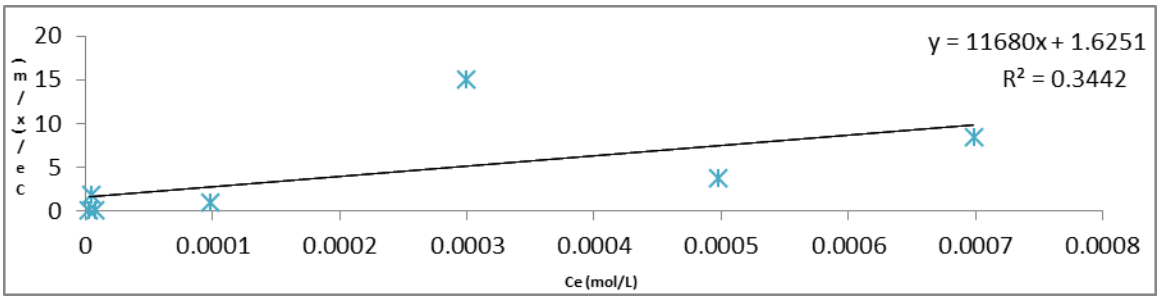

Figure 10: Optimization of Langmuir parameters at temperature 308K of Tea leaves powder

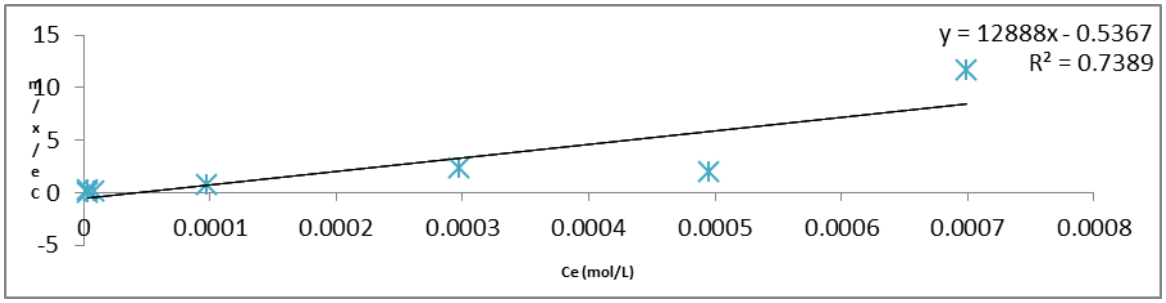

Figure 11: Optimization of Langmuir parameters at temperature 313K of Tea leaves powder

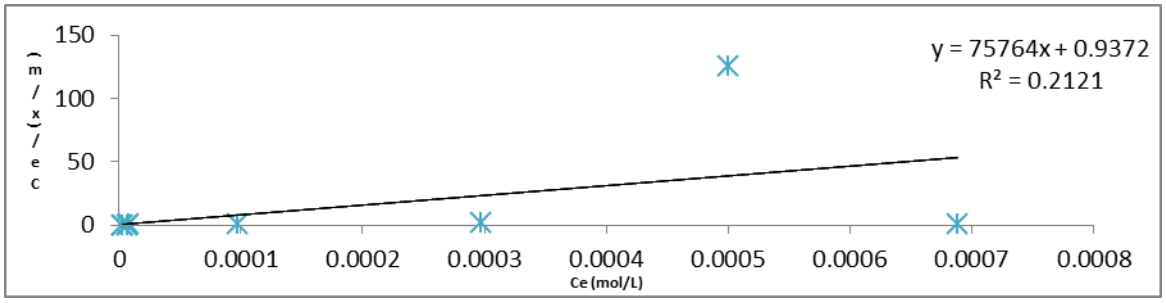

Figure 12: Optimization of Langmuir parameters at temperature 318K of Tea leaves powder

LANGMUIR PARAMETERS OF DATE PITS

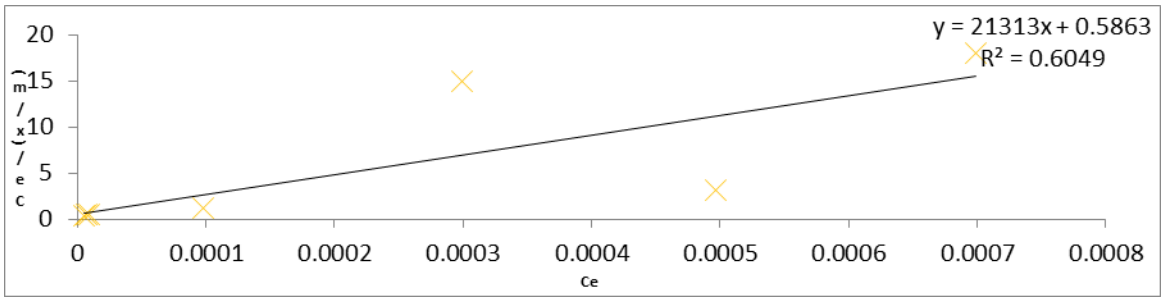

Figure 13: Optimization of Langmuir parameters at temperature 303K of Date pits

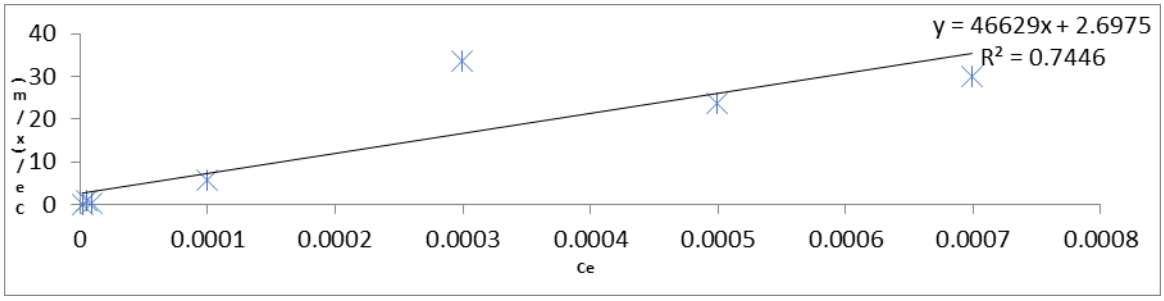

Figure 14: Optimization of Langmuir parameters at temperature 308K of Date pits

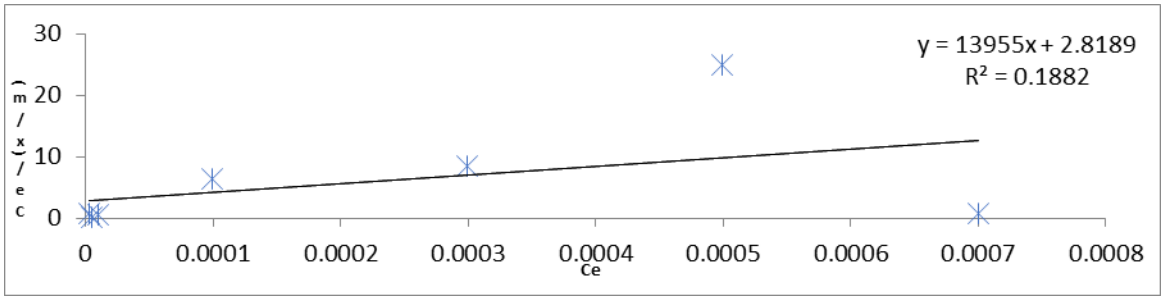

Figure 15: Optimization of Langmuir parameters at temperature 313K of Date pits

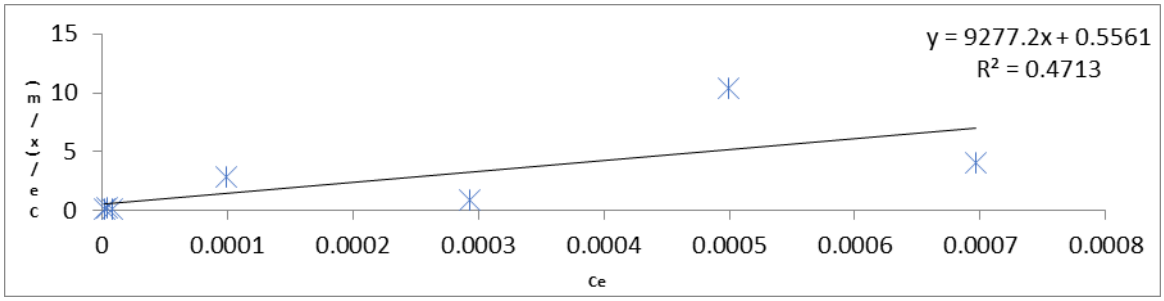

Figure 16: Optimization of Langmuir parameters at temperature 318K of Date pits

LANGMUIR PARAMETERS OF CORN HUSK

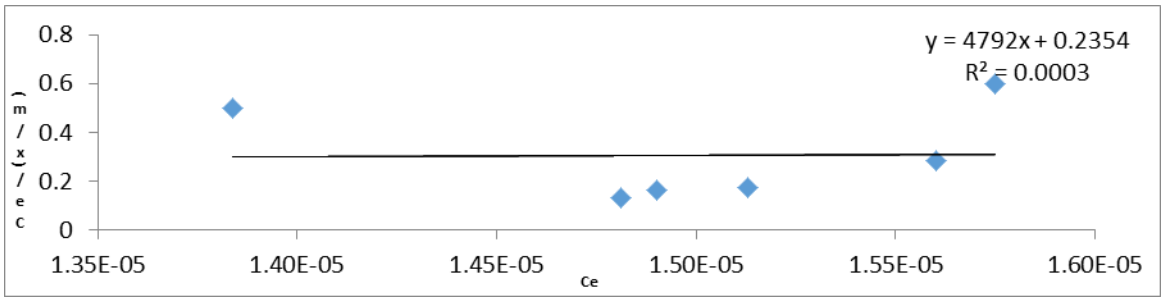

Figure 17: Optimization of Langmuir parameters at temperature 303K of Corn Husk

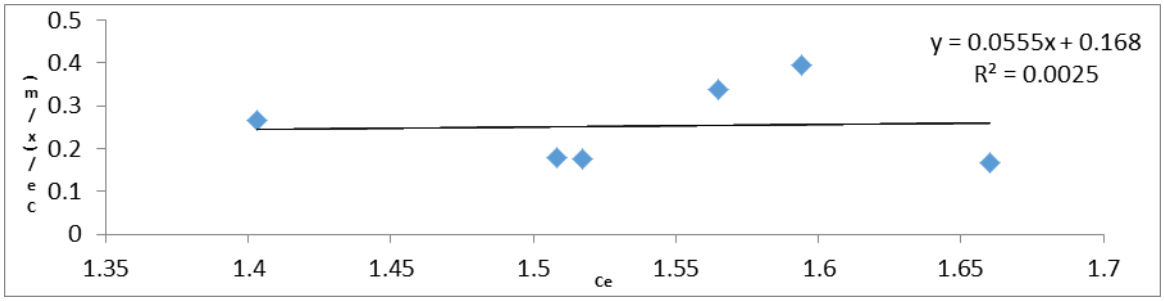

Figure 18: Optimization of Langmuir parameters at temperature 308K of Corn Husk

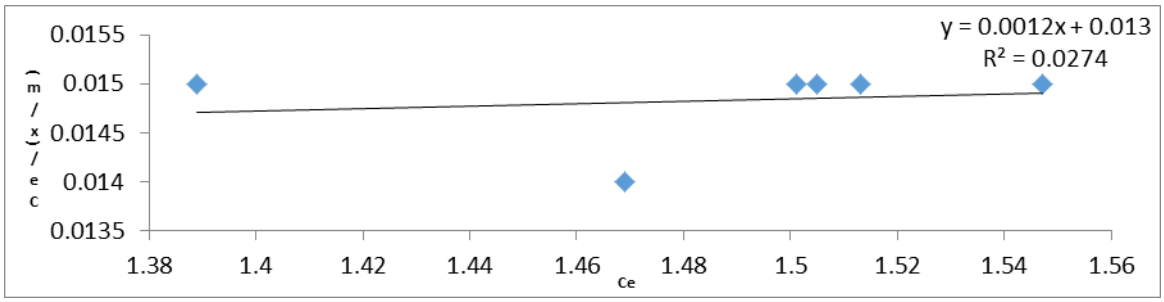

Figure 19: Optimization of Langmuir parameters at temperature 313K of Corn Husk

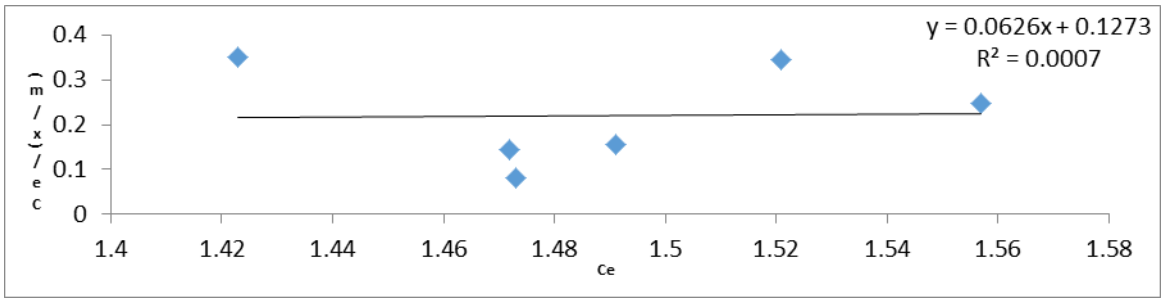

Figure 20: Optimization of Langmuir parameters at temperature 318K of Corn Husk

LANGMUIR PARAMETERS OF PEACH SEEDS

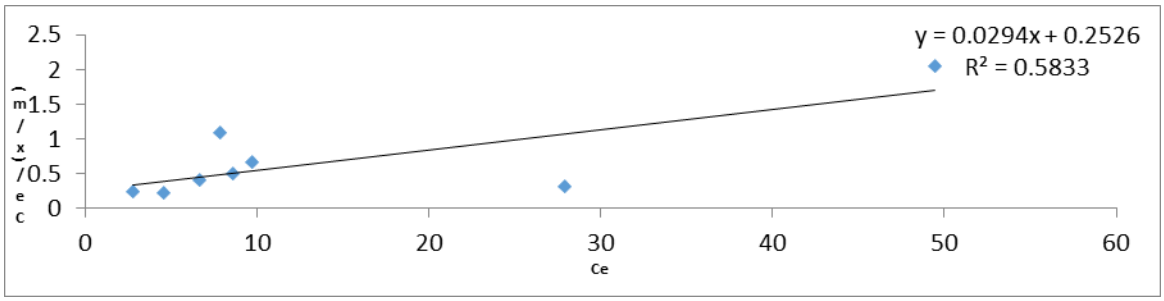

Figure 21: Optimization of Langmuir parameters at temperature 303K of Peach seeds

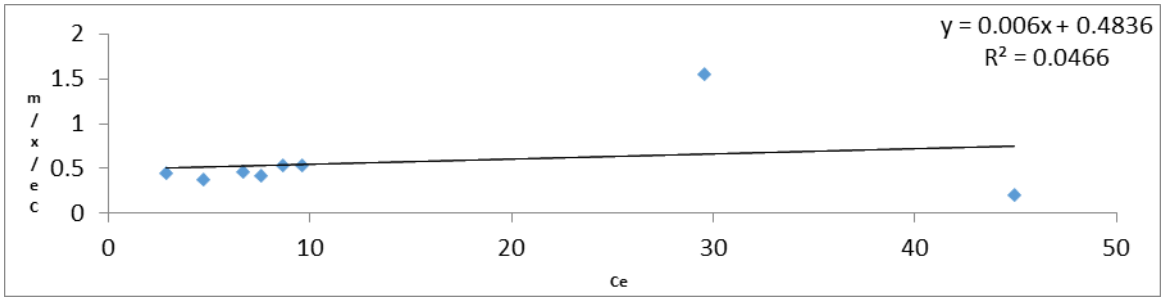

Figure 22: Optimization of Langmuir parameters at temperature 308K of Peach seeds

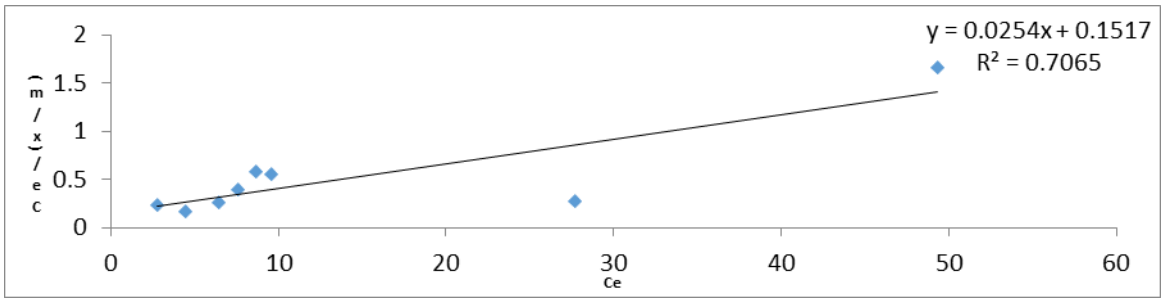

Figure 23: Optimization of Langmuir parameters at temperature 313K of peach seeds

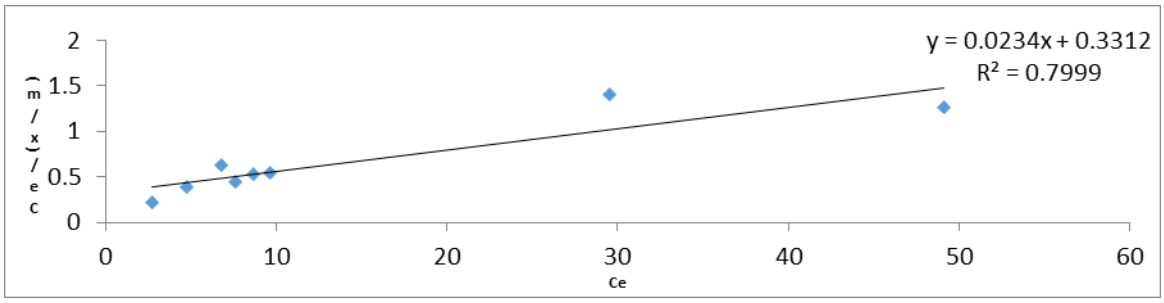

Figure 24: Optimization of Langmuir parameters at temperature 318K of peach seed

FREUNDLICH PARAMETERS OF CORN HUSK

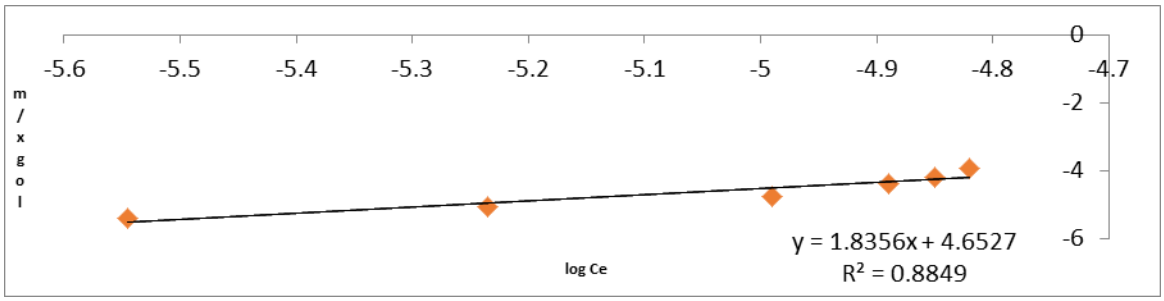

Figure 25: Optimization of Freundlich parameters at temperature 303K of corn husk

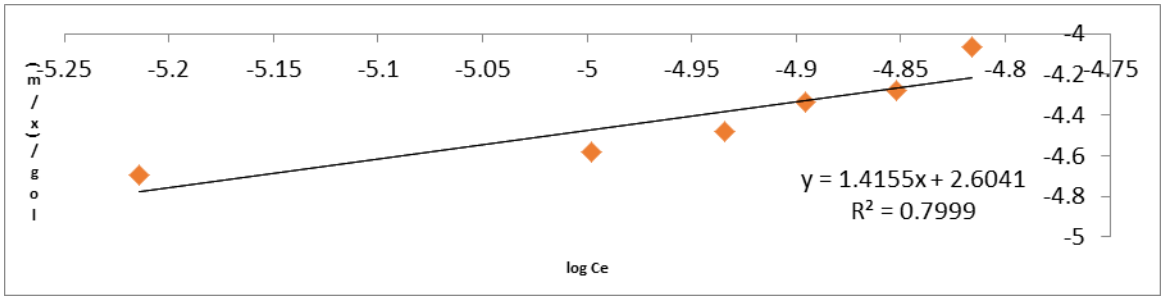

Figure 26: Optimization of Freundlich parameters at temperature 308K of corn husk

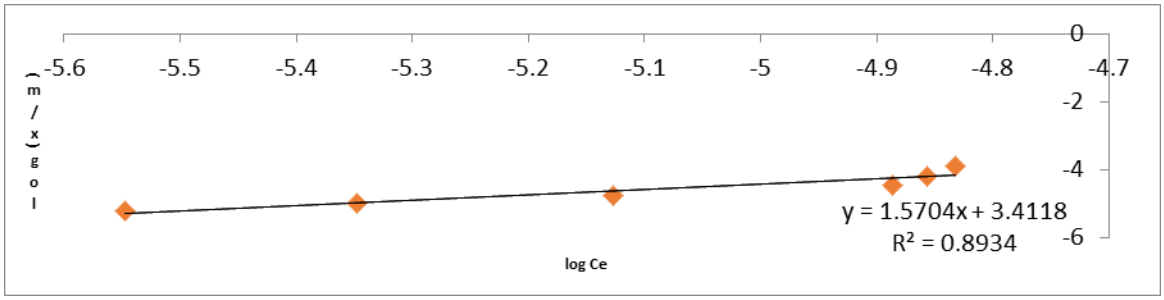

Figure 27: Optimization of Freundlich parameters at temperature 313K of corn husk

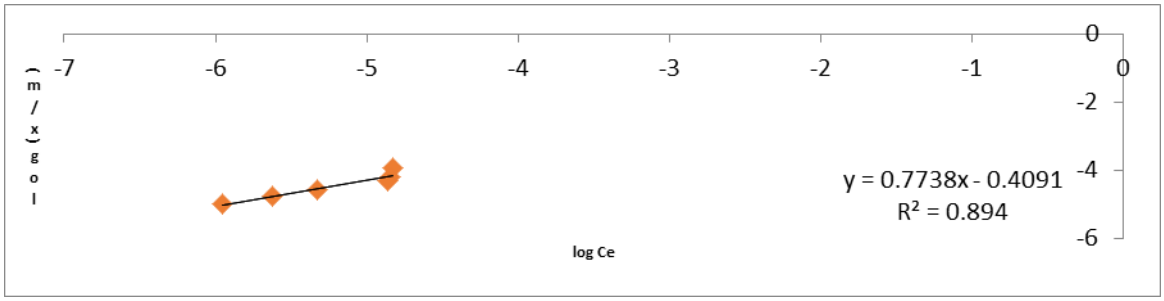

Figure 28: Optimization of Freundlich parameters at temperature 318K of corn husk

FREUNDLICH PARAMETERS OF PEACH SEEDS

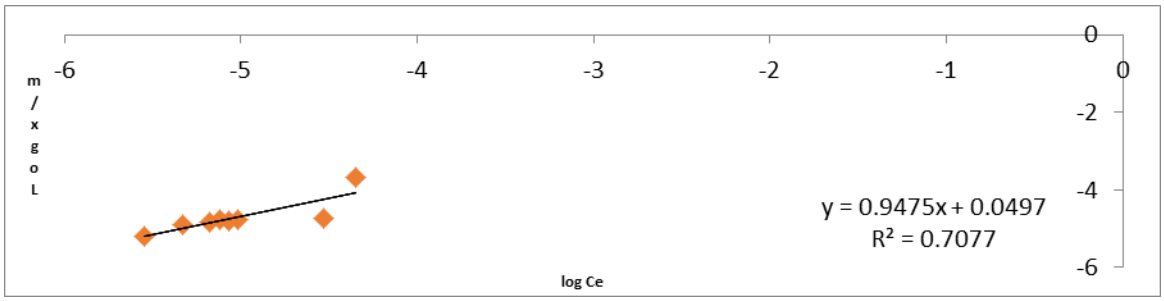

Figure 29: Optimization of Freundlich parameters at temperature 303K of Peach Seeds

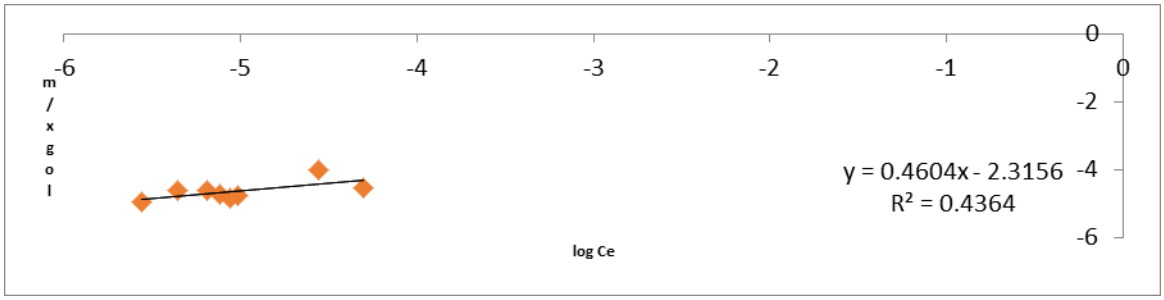

Figure 30: Optimization of Freundlich parameters at temperature 308K of peach seeds

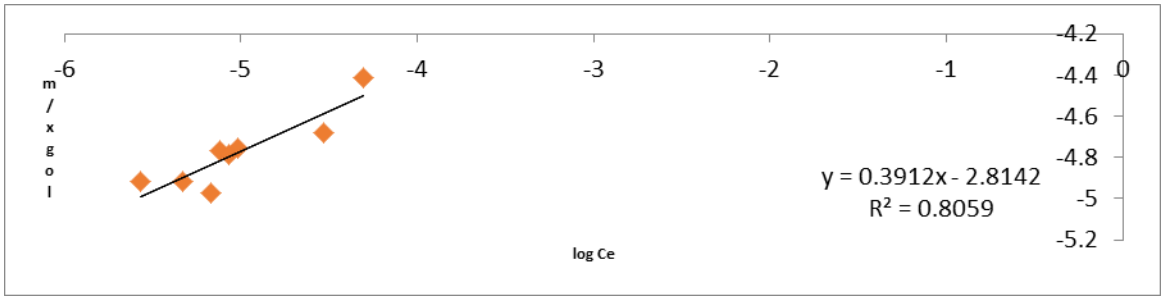

Figure 31: Optimization of Freundlich parameters at temperature 313K of peach seeds

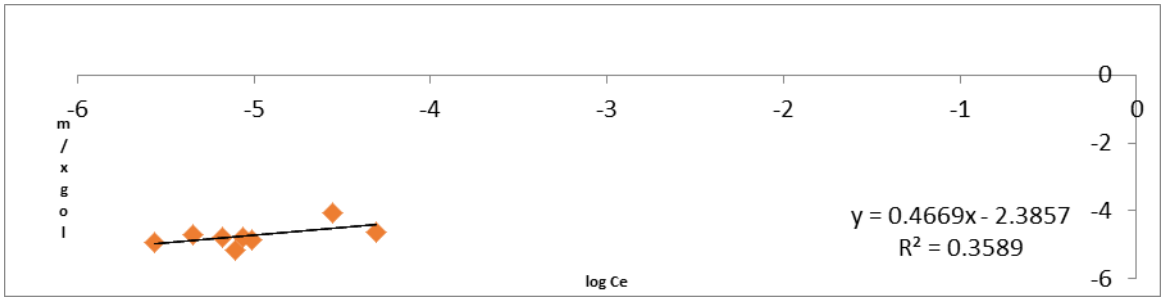

Figure 32: Optimization of Freundlich parameters at temperature 318K of grounded peach seeds

FREUNDLICH PARAMETERS OF DATE PITS

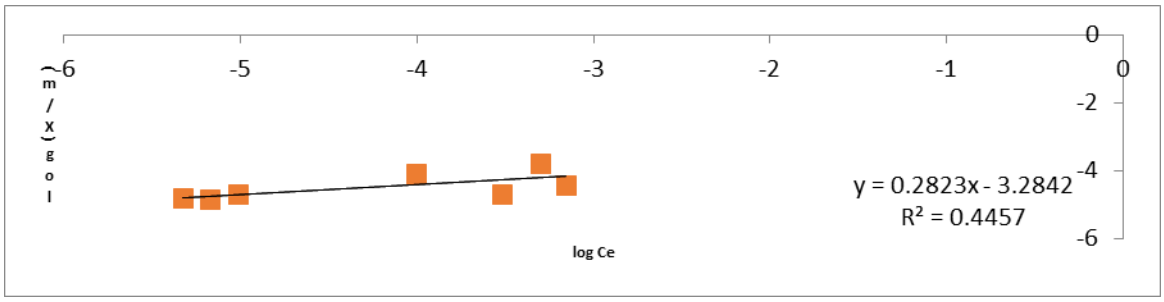

Figure 33: Optimization of Freundlich parameters at temperature 303K of grounded date pits

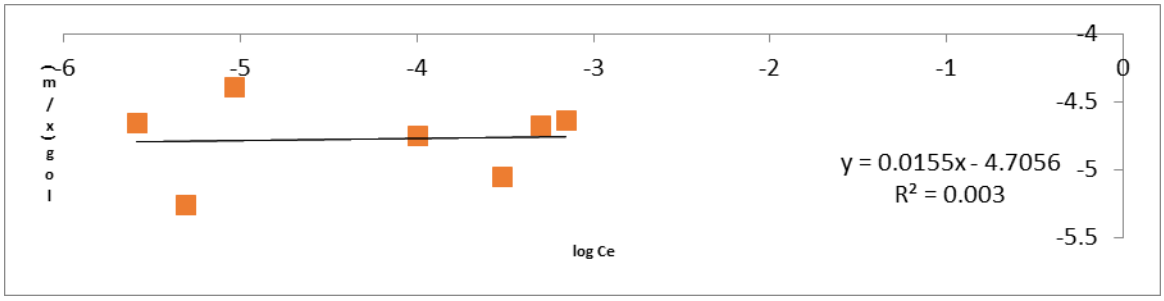

Figure 34: Optimization of Freundlich parameters at temperature 308K of grounded date pits

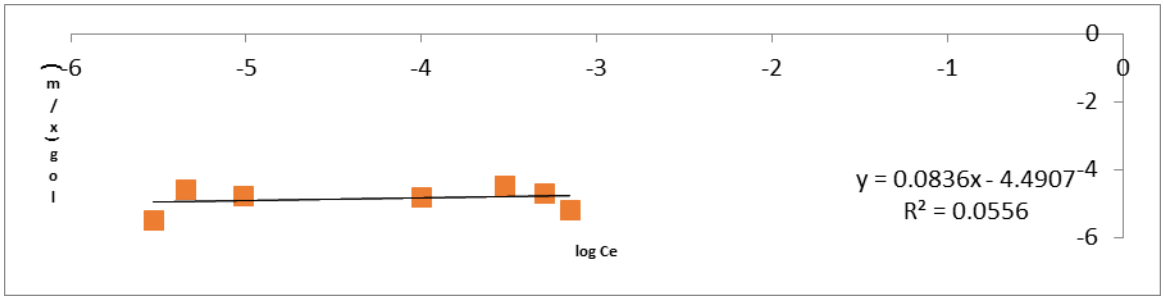

Figure 35: Optimization of Freundlich parameters at temperature 313K of grounded date pits

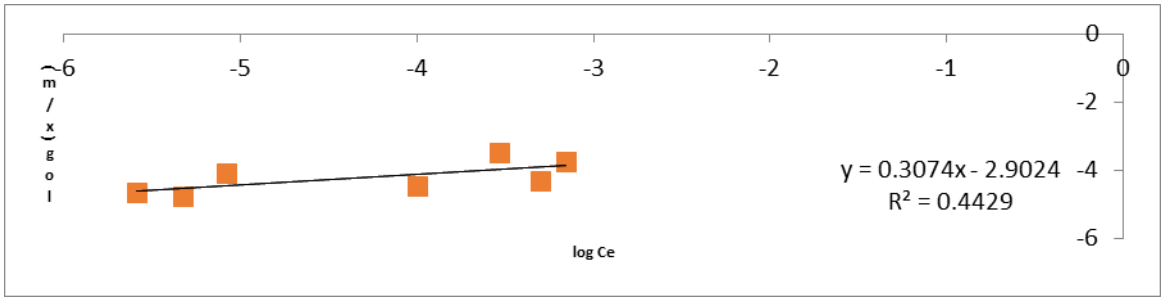

Figure 36: Optimization of Freundlich parameters at temperature 318K of grounded date pits

FREUNDLICH PARAMETERS OF TEA LEAVES

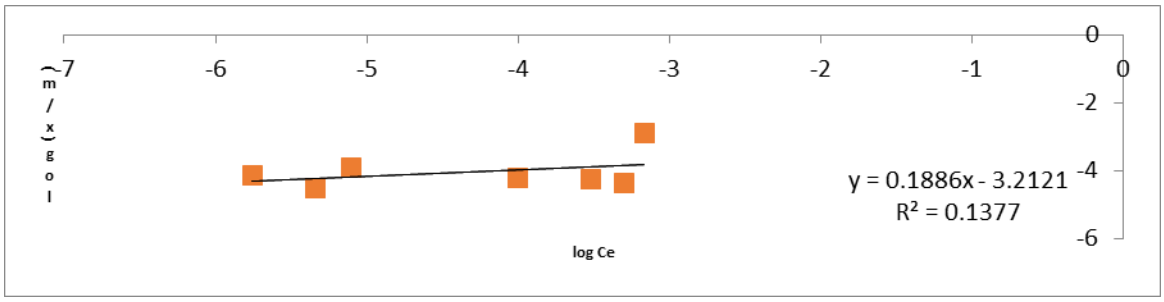

Figure 37: Optimization of Freundlich parameters at temperature 303K of grounded waste of tea leaves

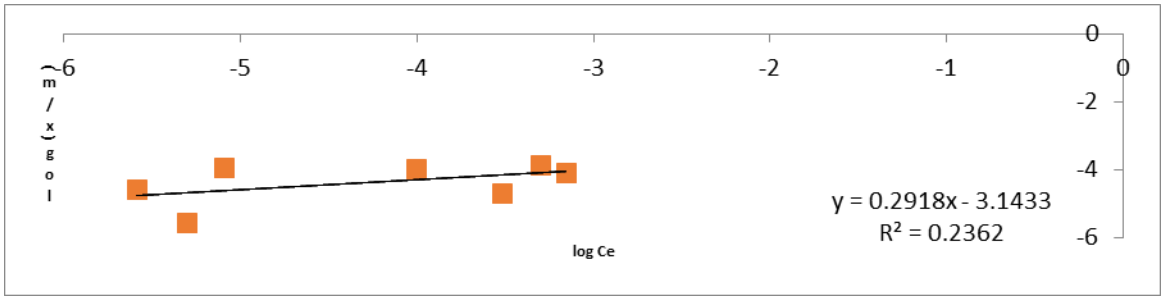

Figure 38: Optimization of Freundlich parameters at temperature 308K of grounded waste of Tea leaves

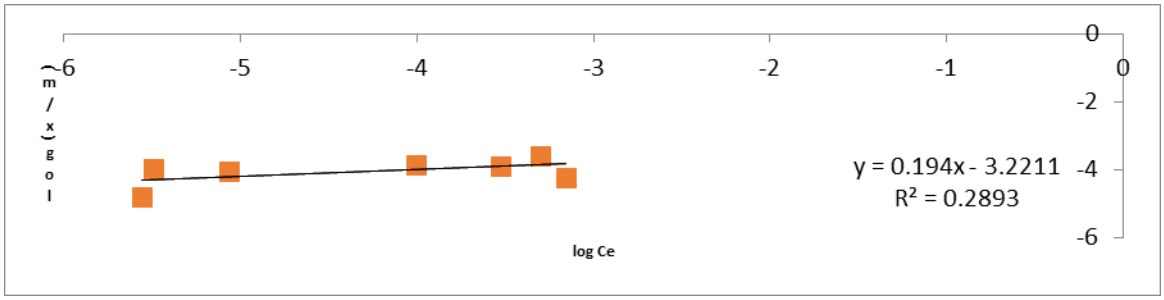

Figure 39: Optimization of Freundlich parameters at temperature 313K of grounded waste of Tea leaves

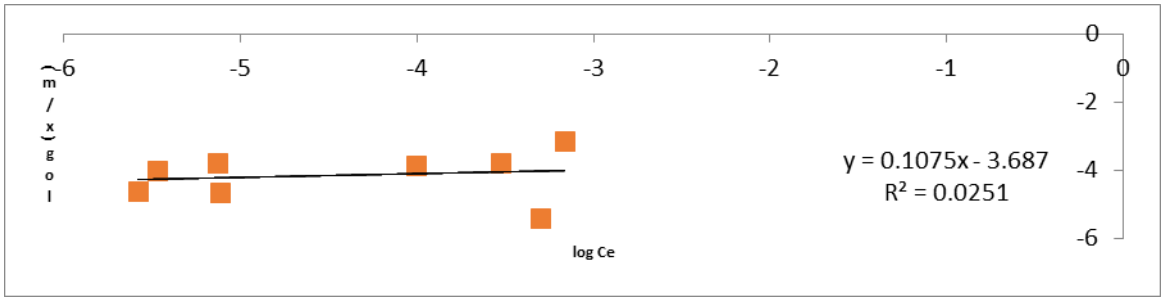

Figure 40: Optimization of Freundlich parameters at temperature 318K of grounded waste of Tea leaves

ADSORPTION KINETICS

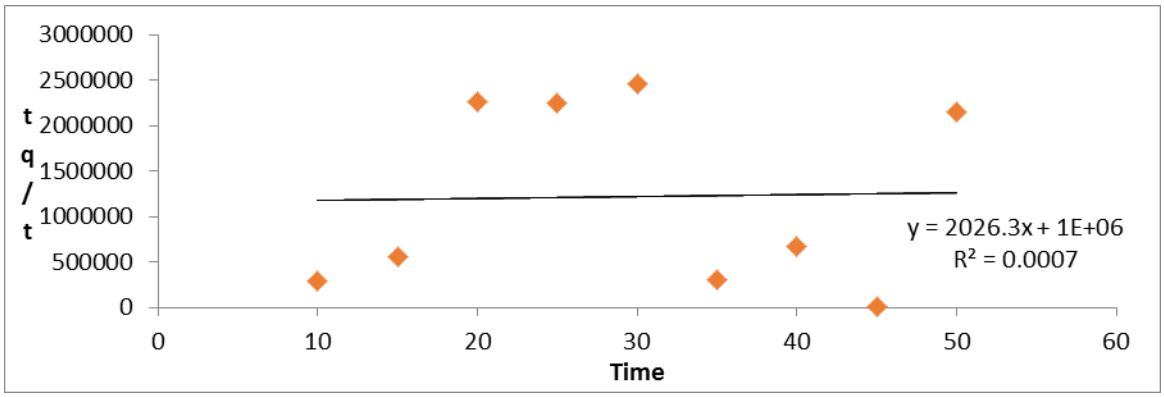

Figure 41: kinetics of date pits by Pseudo -second order

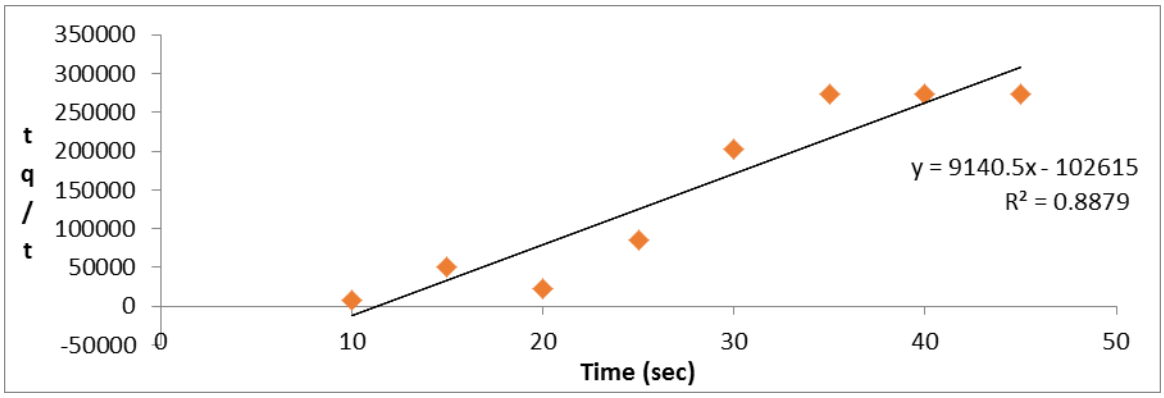

Figure 42: kinetics of tea leaves by Pseudo -second order

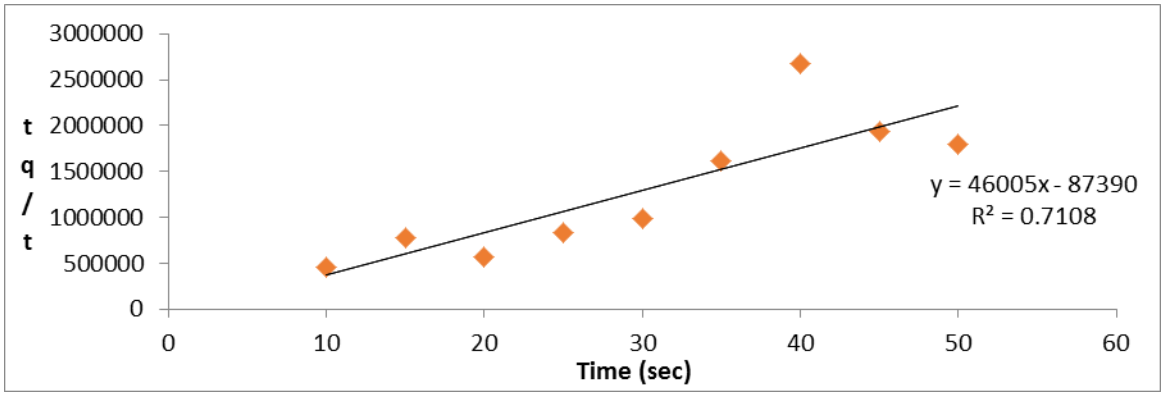

Figure 43: kinetics of peach seeds by Pseudo -second order

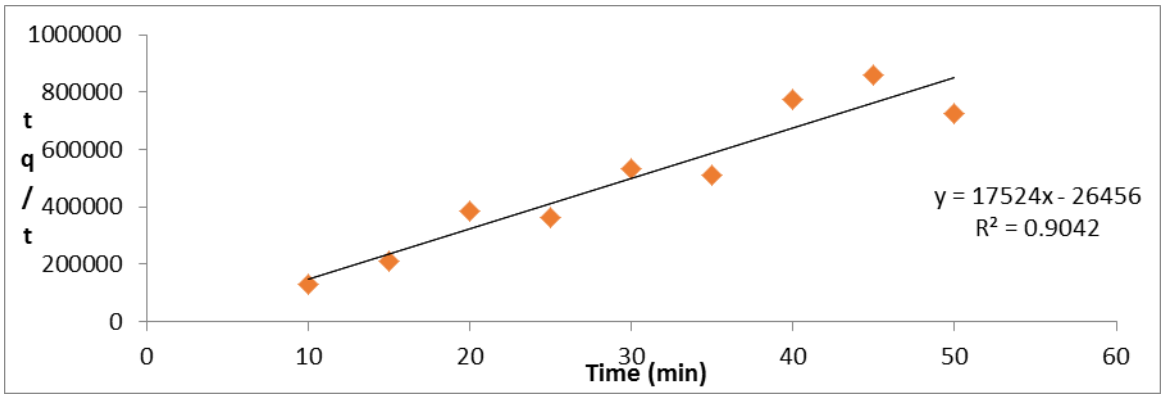

Figure 44: kinetics of corn husk by Pseudo -second order

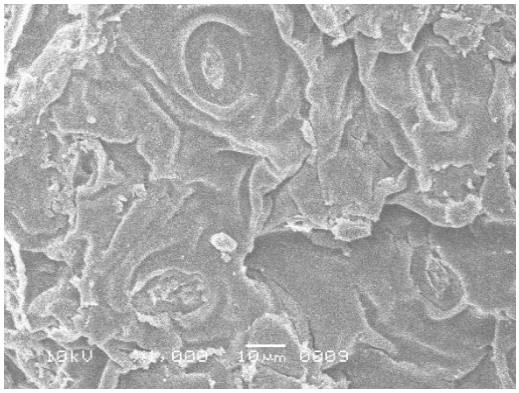

Figure 45: SEM images of tea leaves before adsorption

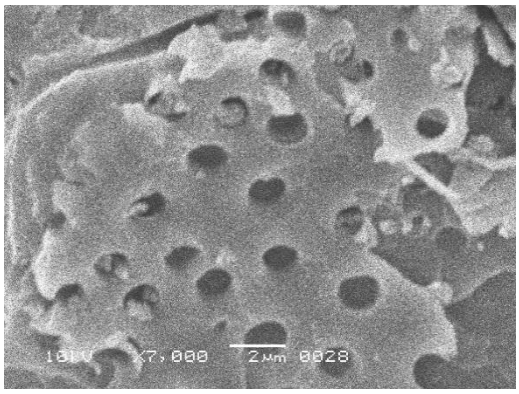

Figure 46: SEM images of tea leaves after adsorption

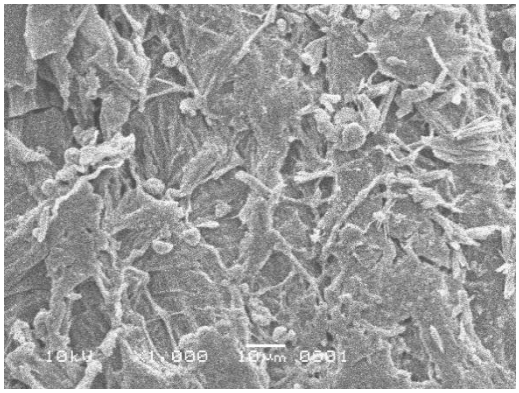

Figure 47: SEM images of corn husk before adsorption

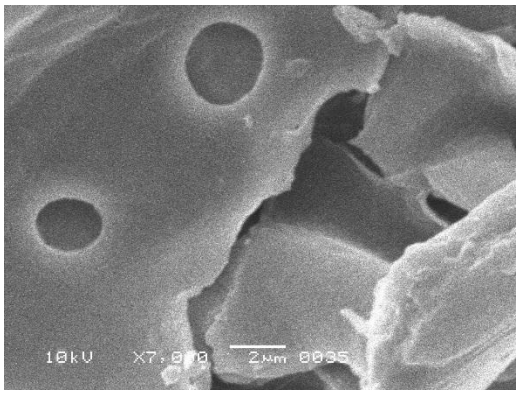

Figure 48: SEM images of corn husk after adsorption

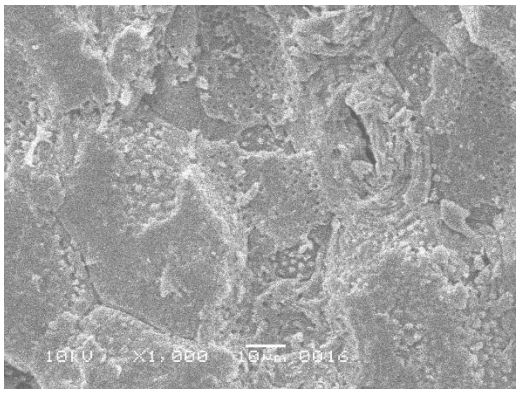

Figure 49: SEM image of peach seed before adsorption

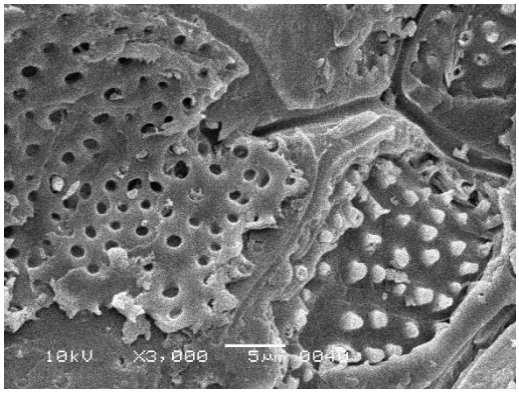

Figure 50: SEM image of peach seed after adsorption

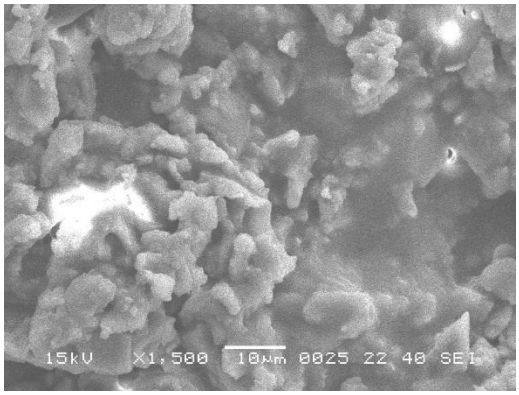

Figure 51: SEM image of Date pits before adsorption

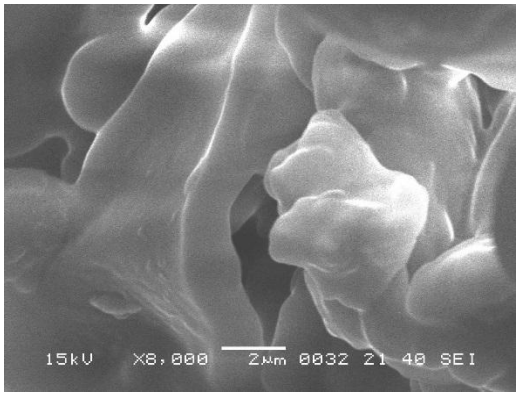

Figure 52: SEM image of Date pits after adsorption

RESULTS AND DISCUSSION

Adsorption of carcinogenic dyes Congo Red (CR) was carried out by tea leaves powder and date pits powder. Adsorption of MGO dye was carried out by peach seeds powder and corn husk powder. Different experiments were performed in the adjusted circumstances of adsorbent's amount in table 1, adsorbents stay time in table 2 and adsorbents were analyzed at different temperatures in table 3. Concentrations of dyes before and after adsorption were recorded by ultraviolet visible spectrophotometer. The structure of natural adsorbents were analyzed by SEM technique from figs. (45-52).

Examination of Effects of Adsorption Parameters on the Adsorption

Effect of Adsorbent's Amount

The optimum amount of adsorbent was taken as 0.4g for tea leaves in figure 1, 0.6g for date pits in figure 2, 0.5 g for corn husk in figure 3 and 0.5g for peach seeds powder in figure 4. By Further increasing of amount of natural bio sorbents did not show any effective removal of dyes as shown in table 1.

Effect of stay time

For tea leaves - congo red system, maximum adsorption was obtained at 35 minutes in figure 5, for date pits – congo red system, maximum adsorption capacity was obtained at 20 minutes in

figure 6, for corn husk- malachite green oxalate system, maximum adsorption capacity was acquired at 30 minutes in figure 7 and for peach seeds – malachite green oxalate system, extreme adsorption capacity was achieved at 15 minutes, as shown in figure 8.

Adsorption Isotherms

Langmuir Adsorption Isotherm

This isotherm shows monolayer adsorption on a consistent surface. Monolayer adsorption must be merely defined by Langmuir adsorption isotherm. Well-known Langmuir equation is as follows:

$$\mathbf{C_e/X/m = 1/KV_m + C_e/V_m}$$

Here, equilibrium concentration is C_e (mol/dm^3), amount adsorbed at equilibrium is X/m (mol/g), intercept is Vm (mol/g) and slope is K (dm^3/mol). Graph with the straight line was assimilated by plotting "C_e/X/m" on y-axis versus "C_e" on x-axis. From the slopes "V_m" and "K" intercepts were studied. The adsorption of Congo Red (CR) and malachite green oxalate (MGO) were examined at different temperatures.

The results indicated that that in case of Tea leaves-Congo red dye system there were decreasing in the values of slope with the increase of temperature from 303K to 313K it proved the strong adsorbate-adsorbent contact at low temperatures. It also revealed that adsorption attraction of dye was dropped with the increased in temperature, therefore adsorption was auspicious at low temperatures. It also prophesied that strong adsorbate-adsorbent attraction occurred at lower temperatures.

The monolayer capacity (V_m), for congo red – tea leaves system formed onto the homogenous adsorbent surface. The value of K was positive presenting that they followed the Langmuir adsorption isotherm. The largest R^2 values of adsorbent-dye endorsed that adsorption happens according to Langmuir isotherm and monolayer forms onto the homogenous adsorbent surface as shown in figs. (9-12).

In the case of Date pits powder-Congo red dye system there was decrease in the values of the Langmuir constant with the increased in temperature from 303K to 318K which showed strong

adsorbate-adsorbent interaction at low temperature. It also proved that attraction of dye reduced with rise in temperature therefore adsorption process was favorable at low temperatures.

Capability of monolayer (V_m), for Congo red – date pits system forms onto the homogenous adsorbent surface. The values of K were positive proved that which followed the Langmuir adsorption isotherm. The largest value of R^2 was 0.7446 obtained at 308K recommended that strong adsorption occurred according to Langmuir adsorption isotherm and monolayer formed onto the homogenous adsorbent surface as shown in figs (13-16).

In Peach seeds powder- Malachite green oxalate dye system there were increased in the values of the Langmuir constant with the increased in temperature from 303K to 318K. It predicted that the strong adsorbate-adsorbent occurred at highest temperature. It also revealed that the adsorption of dye increased with the rise in temperature consequently adsorption was encouraged at high temperature.

The values of K were positive proved that they were followed the Langmuir adsorption isotherm. The largest values of R^2 were 0.7999, 0.7065 and 0.583 at temperature 313K, 308K and 318K respectively showed that the strong adsorption occurred conferring to Langmuir adsorption isotherm and monolayer was formed onto the homogenous adsorbent surface as shown in figs. (21 -24).

In the situation of Corn husk- Malachite green oxalate dye system, values of “K” increase with the increase in temperature from 303K to 318K. It oracles strong adsorbate-adsorbent interaction at higher temperatures. It also disclosed that adsorption of dye increased with increase in temperature so adsorption is encouraging at high temperature.

Monolayer capacity (V_m), for malachite green oxalate – corn husk system formed onto the homogenous adsorbent surface. The values of K were positive offering that they followed the Langmuir adsorption isotherm. The largest values of R^2 was 0.0274 assimilated at 313K confirming that strong adsorption occur according to Langmuir adsorption isotherm and monolayer formed onto the homogenous adsorbent surface as shown in figs. (17-20).

The Freundlich Adsorption Isotherm

This isotherm is specified by the following equation:

$$\mathbf{LogX/m = log\ K + 1/n\ log\ C_e}$$

Values of "K" and "n" were calculated from the intercepts and slopes of their relevant graphs and were written in Tables. Increase in values of constant (K) with the risen in temperature for Congo red dye and malachite green oxalate dye showed that adsorption attraction of both dyes are favorable at higher temperatures [13].

In the case of Tea leaves- congo red system values of constant (K) decreased with the increase in temperature and showed that adsorption of dye was auspicious at lower temperature. With the rise in temperature decrease in the values of (K) occurred which showed there was high interaction with the adsorbent at lower temperature as shown in table (5) and in figs. (46-49). the values of "n" lies in between -1 to10, which showed advantageous effect of the adsorption process. Values of R^2 proved that Freundlich isotherm, which showed formation of multilayer on the surface of adsorbent. The date fitted well in Freundlich isotherm with values of "n" which were 5.3022, 5.4270, 5.15, and 9.30 at temperatures 303K, 308K, 313K and 318 K respectively as shown in figures (37-40).

In the case of Date pits- Congo red system the values of (K) constant decreased with increased in temperature and showed that dye adsorption was auspicious at lower temperature. The decrease the values of K with the increase in temperature showed that there is high interaction with the adsorbent at lower temperature as presented in table (5) and in figs. (42-45). the values of R^2 were nearly about 0.999 showing that the adsorption followed Freundlich isotherm. The data fitted well in Freundlich isotherm with values of "n" 3.54 at 303K and 3.2530 at 318K as shown in figures (33-36).

In the case of Peach seeds- Malachite green oxalate system values of K constants were high at low temperatures which showed that adsorption of the dye was favorable at low temperature. Increase in the values of K with the decrease in temperature showed that there was high interaction with the adsorbent as showed in table (5) and in fig. (38-41). The values of R^2 were 0.707, 0.4364, 0.8059, 0.3589 at temperatures 303K, 308K, 313K and 318K respectively, showing that the adsorption followed Freundlich isotherm. Values of R^2 confirmed the

Freundlich isotherm and showed the formation of multilayer on the surface of adsorbent. The data fitted well in Freundlich isotherm with the values of "n" 1.055, 2.1720, 2.55 and 2.1417 at temperatures 303K, 308K, 313K and 318 K respectively as shown in figures (29-32).

In case of Corn husk- Malachite green oxalate system values of (K) constants decreased with increased in temperatures which offered that adsorption of dye was favorable at low temperature. Decreased in the value of K with the increase in temperature showed that there is high interaction with the adsorbent as presented in table (5) and in fig. (34-37). The values of R^2 were 0.8849, 0.7999, 0.8954 and 0.894 at temperatures 303K, 308K, 313K and 318 K respectively, which showed that the adsorption followed Freundlich isotherm. R^2 proved Freundlich isotherm and specified formation of multilayer on the surface of adsorbent. The data fitted well in Freundlich isotherm with the values of "n" 0.544, 0.70, 0.03 and 1.2923 at temperatures 303K, 308K, 313K and 318 K respectively as shown in figures (25-28).

Influence of Thermodynamic Parameter

Thermodynamic parameters of adsorption progression are used to accomplish the process of spontaneity. Change in Gibb's free energy measures the spontaneity. Its negative value proves the reaction is spontaneous.

ΔH^0, ΔS^0 and ΔG^0 were premeditated by the following equations:

$$\Delta G^0 = \Delta H^0 - T\Delta S^0$$

$$\text{Ln } K_D = \Delta S^0/R - \Delta H^0/RT$$

$$\Delta G^0 = -RT \text{ Ln} K_D$$

Here R, the gas constant, absolute temperature is T, equilibrium constant is K_D. ΔH^0 and ΔS^0 were obtained from slopes and intercepts of "ln K_D" versus 1/T [14].

Negative values of $\Delta G°$ confirms feasibility of method and spontaneity of adsorption with a maximum adsorption of dye. With the increase in temperature decrease in negative value of $\Delta G°$ specifies the adsorption progression of dye is auspicious at greater temperatures. Negative values of $\Delta G°$ and the positive value of $\Delta H°$ for tea leaves, date pits, corn husk proved the spontaneity

of adsorption, whereas peach seeds shown the non-spontaneity of adsorption. Degree of randomness of a system is entropy. ΔS° positive describes structural alterations happen on the adsorbent, and the randomness occurs in the adsorption system. The positive value of ΔH° for date pits, corn husk proved the endothermic nature because there is a large increase of translational mobility on the surface and negative value of ΔH° for peace seeds, tea leaves shown the exothermic process of adsorption. The dye system confirmed (+) values of ΔS^0 describe the randomness and negative values of ΔS^0 indicated some deviation in the adsorption system as shown in table 7.

Kinetics of Adsorption

Linear graph of "t/qt" on y-axis and "t" on x-axis for different concentrations of CR and MGO were plotted which correspond that sorption procedure followed pseudo-second order kinetic as displayed in Figure. qe and qt are the amount of the dye adsorbed on the adsorbent (mol/g) at equilibrium and t is time in minutes, k_2 is the adsorption of second order rate constant (mol/g.min). The correlation coefficients for the second order models are near to 0.999 shows the linearity with high degree of correlation coefficient Study of kinetics of adsorption offers the information regarding the rate of adsorption and practicability of adsorption procedure. The experimental results were pragmatic to examine kinetics by the models of pseudo-second order as shown in table 6 [15].

$$\ln(q_e - q_t) = \ln q_e - k_1 t$$

$$\frac{t}{q_t} = \frac{1}{k_2 q_e^2} + \frac{t}{q_e}$$

The values of R^2 for the MGO sorption on Peach seeds powder and Corn husk powder systems were obtained 0.7108 and 0.9042 as shown in figures (43 and 44) and results of R^2 for CR sorption on Date pits powder and Tea leaves powder were analyzed to be 0.0007 and 0.8879 as shown in figures (41 and 42). Results showed that system followed the pseudo second order kinetics, correlation coefficients for second order models are near 0.999 confirmed linearity with high degree of correlation coefficient.

Where k_{id} is intra-particle diffusion rate constant, which was obtained from slope of the linear plot of "qt" verses" $t_{1/2}$". Intercept contributed the width of boundary layer i.e. greater intercept; the enhanced will be border layer effect. Positivity of slope expressed controlled adsorption process. Date pits powder, tea leaves powder, Peach seeds powder showed positive slope whereas corn husk exhibited negative slope as shown in table 6.

SEM Interpretations of Natural particles

Top characterization techniques is SEM. The scanning electron micrograph specifies that the particles are quite homogenous in nature and the size ranging from 50 - 120nm for natural bio sorbents. After the adsorption of tea leaves, date pits, corn husk and peach seed powder, the diameter of all the natural adsorbents were decreased because the dye coated onto their surfaces as shown in figures from 45 to 52 [16].

Conclusion

For the elimination of chemical toxins from water and waste water only adsorption is the familiar, effective and cheap method that yields high-quality results. The present research emphasizes on the removal of contaminants by using adsorption process with the collection natural adsorbents.

Different natural adsorbents like date pits, tea leaves, corn husk and peach seeds were used. The characterization of natural adsorbents characterization were analyzed by SEM. Malachite green oxalate dye adsorption was calculated and analyzed by using corn husk and peach seeds particles working as adsorbent under various conditions. Similarly adsorption of Congo red dye was considered by using waste tea leaves and date pits particles. The optimum circumstances for the adsorption of dyes adsorbents were presented. Investigational data presented adsorption followed the pseudo second order kinetics. Experimental data was form fitted well in Freundlich and Langmuir isotherms. After analyzing all the graphs and data it was concluded that Freundlich isotherm form fitted well approximately to all investigational adsorption data, and was particularly outstanding for extremely heterogeneous adsorbents. The negative value of ΔG^o proved the spontaneity of adsorption of waste tea leaves powder, date pits powder and corn husk powder. The positive ΔG^o value of Peach seeds powder confirmed non-spontaneity of the

adsorption. The maximum removal of dyes by experimental results were found and it was concluded that this specific method could be employed on industrial scale for waste minimization. All natural adsorbents particles proposed a lot of auspicious benefits in the forthcoming era.

Treatment of dyes using fresh seeds powder was a highly economic and simple method than other methods meanwhile it has an excellent capability of eliminating color. Contaminated dyes which contaminate huge part of textile emission can be distorted into dull and non-toxic composites by this method. Hence, it is applicable for industrial pollutants for improving the worth of wastewater of fabric industries and numerous others. Furthermore effort for obtaining other constraints of dye waste using the mentioned method can be conceded out to develop the adsorption proficiency.

REFERENCES

1. Ho, Y.S. (2015), Comment on “Genetic characterization, nickel tolerance, biosorption, kinetics, and uptake mechanism of a bacterium isolated from electroplating industrial effluent”. *Canadian Journal of Microbiology*, **61** (11), 881-882.
2. Atiya Firdous and Uzma Hameed, The synthesis and characterization of nano composites of CdO and its applications for the treatment of simulated dye waste water. American chemical science Journal, 2016,13(1);1-10, ACSJ.23799.
3. Balaz, M., Bujnakova, Z., Balaz, P., Zorkovska, A., Dankova, Z. and Briancin, J. (2015), Adsorption of cadmium (II) on waste biomaterial. *Journal of Colloid and Interface Science*, **454**), 121-133.
4. Mahmoodi, N.M. and Masrouri, O. (2015), Cationic Dye Removal Ability from Multicomponent System by Magnetic Carbon Nanotubes. *Journal of Solution Chemistry*, **44** (8), 1568-1583.
5. Smart Platform for Hyperthermia Application in Cancer Treatment: Cobalt-Doped Ferrite Nanoparticles Mineralized in Human Ferritin Cages. ACS Nano, 2014, 8 (5), pp 4705–4719

6. Ho, Y.S. (2015), Comments on "Isothermic and Kinetic Modeling of Fluoride Removal from Water by Means of the Natural Biosorbents Sorghum and Canola". *Fluoride*, **48** (3), 266-268.
7. Jia, A.Y., Wu, C.D., Hu, W.C. and Hu, C.X. (2015), Bromate Adsorption on Three Variable Charge Soils: Kinetics and Thermodynamics. *Clean-Soil Air Water*, **43** (7), 1072-1077.
8. Santos, S.C.R. and Boaventura, R.A.R. (2015), Treatment of a simulated textile wastewater in a sequencing batch reactor (SBR) with addition of a low-cost adsorbent. *Journal of Hazardous Materials*, **291**), 74-82.
9. Mahmoodi, N.M. and Ghobadi, J. (2015), extended isotherm and kinetics of binary system dye removal using carbon nanotube from wastewater. *Desalination and Water Treatment*, **54** (10), 2777-2793.
10. Liu, S.J. (2015), a mathematical model for competitive adsorptions. *Separation and Purification Technology*, **144**), 80-89.
11. Mahmoodi, N.M. and Maghsoodi, A. (2015), Kinetics and isotherm of cationic dye removal from multicomponent system using the synthesized silica nanoparticle. *Desalination and Water Treatment*, **54** (2), 562-571.
12. Ho, Y.S. (2015), Comments on "Synthesis and Adsorption of Ni (II) on Ni (II)-Imprinted Polyaniline Supported on Attapulgite Modified with 3-Methacryloxypropyltrimethoxysilane". *Adsorption Science & Technology*, **33** (4), 427-428.
13. Mariappan, R., Vairamuthu, R. and Ganapathy, A. (2015), Use of chemically activated cotton nut shell carbon for the removal of fluoride contaminated drinking water: Kinetics evaluation. *Chinese Journal of Chemical Engineering*, **23** (4), 710-721.
14. Zhao, J.M., Hu, Q.Y., Li, Y.B. and Liu, H.Z. (2015), efficient separation of vanadium from chromium by a novel ionic liquid-based synergistic extraction strategy. *Chemical Engineering Journal*, **264**), 487-496.
15. Bhatt, R., Sreedhar, B. and Padmaja, P. (2015), Adsorption of chromium from aqueous solutions using cross linked chitosan-diethylene triamine penta acetic acid. *International Journal of Biological Macromolecules*, **74**), 458-466.
16. Ong, S.A., Ho, L.N., Wong, Y.S. and Zainuddin, A. (2013), Adsorption Behavior of Cationic and Anionic Dyes onto Acid Treated Coconut Coir. *Separation Science and Technology*, **48** (14), 2125-2131.

600